A nonsynaptic mechanism underlying interictal discharges in human epileptic neocortex

Anita K. Roopun[a], Jennifer D. Simonotto[b], Michelle L. Pierce[a], Alistair Jenkins[c], Claire Nicholson[c], Ian S. Schofield[c], Roger G. Whittaker[a], Marcus Kaiser[a,b,d], Miles A. Whittington[a], Roger D. Traub[e], and Mark O. Cunningham[a,1]

[a]Institute of Neuroscience, The Medical School, Framlington Place, Newcastle University, Newcastle-upon-Tyne NE2 4HH, UK; [b]School of Computing Science, Claremont Tower, Newcastle University, Newcastle-upon-Tyne NE1 7RU, UK; [c]Regional Neurosciences Centre, Newcastle General Hospital, Newcastle-upon-Tyne NE4 6BE, UK; [d]Department of Brain and Cognitive Sciences, Seoul National University, Seoul 151-746, Korea; and [e]IBM T.J. Watson Research Center, Yorktown Heights, NY 10598

Very fast oscillations (VFOs, >80 Hz) are important for physiological brain processes and, in excess, with certain epilepsies. Putative mechanisms for VFO include interneuron spiking and network activity in coupled pyramidal cell axons. It is not known whether either, or both, of these apply in pathophysiological conditions. Spontaneously occurring interictal discharges occur in human tissue in vitro, resected from neocortical epileptic foci. VFO associated with these discharges was manifest in both field potential and, with phase delay, in excitatory synaptic inputs to fast spiking interneurons. Recruitment of somatic pyramidal cell and interneuron spiking was low, with no correlation between VFO power and synaptic inputs to principal cells. Reducing synaptic inhibition failed to affect VFO occurrence, but they were abolished by reduced gap junction conductance. These data suggest a lack of a causal role for interneurons, and favor a nonsynaptic pyramidal cell network origin for VFO in epileptic human neocortex.

epilepsy | fast ripple oscillation | ripple oscillation

Advances in electroencephalogram (EEG) techniques have revealed a much larger *temporal* window of oscillatory activity exists than has been previously thought (1–4). Of particular interest are very fast oscillations (VFOs), lying outside the traditional EEG frequency bands (5). These oscillations, at frequencies over c.80 Hz, are readily observable in animal models of epilepsy in vivo (6, 7), in vitro (8, 9), and clinically (10–14). In the epileptic human brain, VFOs are seen in structures involved in the pathology of temporal lobe epilepsy (TLE) (10, 15–18).

Although VFOs are seen in epileptic tissue, similar, transient expression of VFOs is also seen in normal cortex, albeit at lower power. As part of "physiological sharp waves," brief ripples of VFOs at c.200 Hz are seen and are suggested to be involved in the time-compressed replay of previous spike sequences in principal cells (19). A number of putative mechanisms of generation exist: Initial observations in vivo showed that principal cell unit activity was low during sharp waves, but that certain fast spiking (FS) interneurons were capable of spiking at VFO frequencies immediately before and sometimes during the event (20, 21). In vitro observations showed a predominantly inhibitory somatic input to principal cells during sharp waves (22). These observations suggest a role for rapid discharges from inhibitory interneurons as causal for the sharp wave and possibly the accompanying VFO. However, other studies have shown that brief VFO discharges in nonepileptic tissue survive synaptic blockade in low calcium ion-containing media (23), with principal cell spikelets, rather than full spikes manifest as units, being generated at VFO frequency. Computational modeling predicted that VFO was generated as an emergent property of gap-junctionally coupled axons forming a plexus driven by ectopic action potential generation (24). This form of network is the only one to date shown to support frequencies as high as those seen in sharp waves (25), but despite the recent ultrastructural demonstration of gap junctions between axons (26) the existence of such an axonal network remains controversial.

Whereas no definitive evidence exists to support a single mechanism of generation of physiological sharp waves, the situation regarding VFO in epileptic tissue is even more equivocal. Despite superficial similarities, it is not clear whether the VFO seen in interictal discharges has the same structure as physiological sharp waves. A semantic separation between VFO associated with sharp waves and that associated with ictal and interictal activity—pathological high-frequency oscillations (pHFOs)—is noted. Staba et al. (13) highlighted the presence of two distinct frequency bands in the VFO range. The first, termed the "ripple" band (80–140 Hz), may be analogous to VFOs seen under physiological conditions (10, 11, 20, 27). The second, termed the "fast ripple" band (170–355 Hz), has been reported to occur overtly at seizure foci in patients with TLE (13, 15–18). A number of studies using subdural grid electrodes (17, 18, 28–30), depth macro- (14, 31, 32), and microelectrodes (33) have also reported a high correlation between VFO/pHFOs and regions of seizure onset. As far as a mechanism is concerned, in vivo recordings again show correlation between field VFO transients and interneuron unit activity (34), but in vitro studies suggest a primary causal role for gap-junctionally coupled principal cell axons (35).

To attempt to resolve these issues, we investigated the relationship between synaptic inhibition and VFO generation during spontaneous interictal discharges in vitro in neocortical slices from epileptic patients and in a detailed cortical column computational model. The data showed that interictal discharges are manifest in very small volumes of tissue and, whereas interneuron outputs can be recruited during these interictal events, the VFO was only abolished by manipulations that target gap junction-mediated intercellular communication.

Results

Forty-one slices from epileptic temporal cortex were acquired from 11 subjects (Table S1), where prior EEG and electrocorticography recordings suggested that resected cortical tissue was at least part of a region which generated seizure activity. A broad range of primary pathologies was included, as it has been suggested that VFO/pHFO is a ubiquitous feature of neocortical epileptic foci (36). Intracranial foramen ovale (FO) electrode recordings from the mesiobasal aspect of the temporal lobes revealed regular interictal spike discharges that contained VFO (Fig. 1*Ai*). These spontaneous interictal events resembled spike and wave discharges with a brief (80–160 ms) burst of VFO at onset
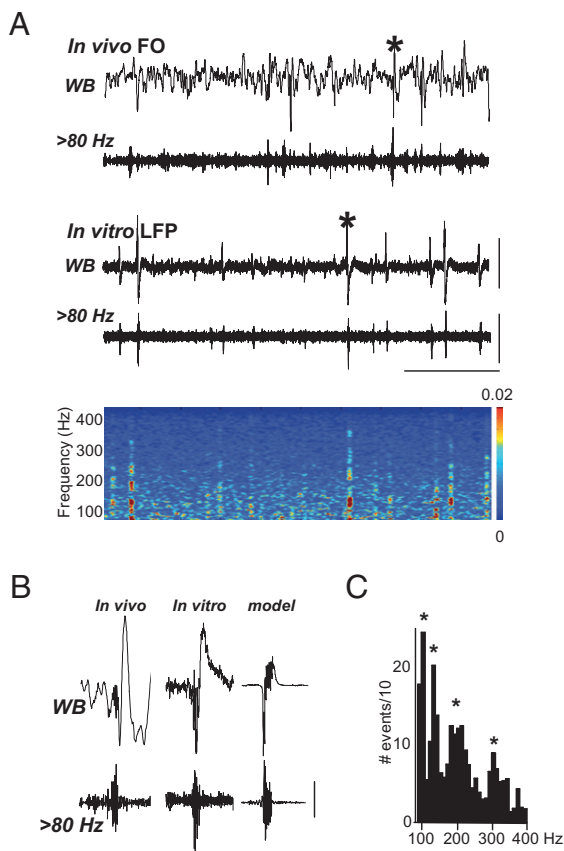
Fig. 1. Spontaneous very fast oscillations (VFOs) are generated in human temporal neocortical slices in vivo and in vitro. (*A*) FO electrodes implanted in patient 1, who presented with right medial temporal lobe sclerosis, demonstrate spike and wave interictal events in a wide-band (WB) recording. The band pass filtered trace (20 s duration) illustrates that oscillatory activity above 80 Hz is observed coincidently with the sharp wave complex. In vitro LFP recordings in slices of superior mediotemporal cortex (20 s duration) resected from the same patient demonstrated spontaneous sharp wave interictal discharges. Band pass filtered trace reveals VFO behavior strongly associated with sharp wave discharges, as can be seen in the spectrogram of the activity illustrated. (*B*) Comparison of two selected events [denoted by asterisks in (*A*)] from in vivo FO and in vitro LFP—inverted for reference to the far field potential FO data—recordings reveal a similar location of the VFO activity at the initial stage of the sharp wave event. The cortical column model, containing all synaptic and gap junctional connections, reproduced the VFO and the initial low-frequency envelope of the interictal discharge with high fidelity. (*C*) Histogram displays the total number of detected VFO events from 80 to 400 Hz ($n = 20$, epochs of data = 60 s). Bin width of histogram was 5 Hz. [Scale bars, (*A*) 500 μV (upper), 200 μV (lower), 5 s; (*B*) 200 μV (in vivo trace), 100 μV (in vitro trace). Scale bars for the model "field" are arbitrary.]

(Fig. 1*B*). Events with similar appearance were seen spontaneously in extracellular recordings in vitro, with an interevent interval of 1.8 ± 0.2 s ($n = 20$), in 20 slices from 11 subjects (Fig. 1*Aii*). As with the FO recordings, these interictal events had VFO present at their onset, with an overall mean duration of 126 ± 8 ms ($n = 20$). FO, extracellular in vitro, and cortical column model data all showed overt transients of VFO and broadly similar initial portions of the interictal spike envelope (Fig. 1*B*). As with previous observations of VFO in human epilepsy, these events appeared to be composed of multiple frequencies (15, 16). Using automated detection, the frequencies within VFOs ranged from 85 Hz to 492 Hz, with a median value of 215 Hz. Within this range, four modal peak frequency bands were seen (Fig. 1*C*). Postsurgical follow-up revealed that 10/11 patients who donated tissue had a reduction or abolition of seizure activity, indicating that the tissue studied

formed at least part of the seizure onset zone. Extracellular recordings from control temporal cortex, prepared and maintained in an identical manner, acquired from nonepileptic patients ($n = 7$; see *Methods*), did not demonstrate any spontaneous interictal or sharp wave-like events in any slices tested.

To test the role of GABA$_A$ receptor-mediated synaptic inhibition in interictal discharges and accompanying VFO, we bath applied a low concentration of gabazine (500 nM) to reduce inhibition [by c.80% (37)] without generating spontaneous ictal-like events. Under control conditions, epochs of VFO were seen with slower interictal spike envelopes of widely varying amplitudes (Fig. 2*A*). Upon wash-in of gabazine, these slow components of the interictal discharge were reduced in power by $85 \pm 7\%$ (Fig. 2*B*). However, brief VFO discharges persisted and mean VFO power per discharge was not significantly changed ($105 \pm 12\%$, $P > 0.05$ cf control). Reduction in synaptic inhibition (but not synaptic activation of interneurons) also had no discernible effect on the brief epochs of VFO generated by the computational model (Fig. S1*A*). Reducing inhibitory postsynaptic currents (IPSCs) by 95% did not change the "field" discharge shape or the somatic spike patterns in LV neurons and FS interneurons, despite the large drop in perisomatic inhibition of these cells (cf. Fig. S1 *A* and *B*). These data and simulations suggested that, whereas synaptic inhibition shaped the slow envelope of the interictal discharge as a field potential phenom-
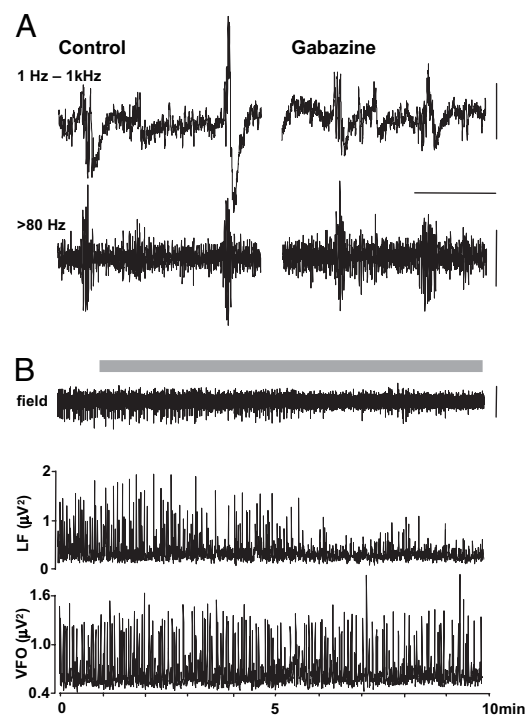

Fig. 2. Spontaneous VFOs are preserved under conditions of reduced cortical inhibition. (*A*) Example wide-band recordings (1 Hz–1 kHz) and the high pass filtered (>80 Hz) equivalent in both control conditions and in the presence of the specific GABA$_A$ receptor antagonist, gabazine (500 nM). The example traces show one epoch with two events in each condition. Note the variable amplitude of the lower-frequency envelope around VFO in the control data. Gabazine abolished the large-amplitude slow envelope but not the VFO. (*B*) Direct comparison of the interictal event proper and the VFO component of the extracellular record during gabazine wash-in. Grey bar denotes presence of 500 nM gabazine in the bathing medium. The plots below denote the instantaneous peak amplitude value (for 200 ms sliding-windowed spectra) for low-frequency envelope of the interictal event (<20 Hz, LF) and the VFO itself (>80 Hz, VFO). [Scale bars, (*A*) 200 μV (upper), 100 μV (lower), 300 ms; (*B*) 200 μV.]

enon, it was not required for generation of the VFO itself. To examine the contribution of depolarizing GABA in the generation of interictal discharges, we bath applied the selective NKCC1 antagonist bumetanide (10 μM), which negatively shifts E_{GABA} and is known to suppress interictal behavior in vitro in human epileptic subicular slices (38). Application of bumetanide ($n = 2$) for periods of >30 min (period required to obtain a new steady-state level of internal Cl$^-$) produced no reduction ($P > 0.05$) in the interevent interval for spontaneous interictal events (control patient 1, 0.69 ± 0.30 s, bumetanide, 0.77 ± 0.30 s; control patient 9, 1.83 ± 0.10 s, bumetanide, 2.60 ± 0.30 s).

Intracellular recordings from LIII pyramidal neurons were then performed to quantify the apparent lack of relationship between single-cell inhibitory postsynaptic potentials (IPSPs) and field VFO power under control conditions. In particular, we wished to find intracellular correlates for the highly variable nature of the relationship between VFO/pHFO and the slower field envelope characterizing some of the interictal events (Fig. 3Ai). Mean IPSP amplitude during interictal events was 4.8 ± 0.3 mV ($n = 116$ events from 4 pyramidal cells from patients 7–10). The field VFO power showed less variability with a mean power per event of 0.219 ± 0.006 μV^2. IPSPs were recorded at membrane potentials from −55 to −60 mV and showed no significant relationship, in terms of amplitude, to the accompanying field VFO ($R^2 = 0.001$). Indeed, 18/116 bursts of VFO had no discernible accompanying IPSP (Fig. 3B). A similar lack of relationship between VFO field power and excitatory synaptic inputs (EPSPs) to pyramidal cells was also seen. Mean EPSP amplitude during interictal events was 2.6 ± 0.3 mV ($n = 126$ events from 4 cells), and mean field VFO power was 0.191 ± 0.007 μV^2. At membrane potentials ranging from −55 to −65 mV, pyramidal neuron EPSPs were quantified during 126 interictal events in 4 slices from 4 patients. There was no significant correlation between EPSP amplitude and VFO power ($R^2 = 0.003$) (Fig. 3B). The number of interictal discharges containing VFO that were not accompanied by any discernible EPSP intracellularly was much higher than for IPSPs (39/126). Figure 3Aii shows two such consecutive EPSP "failures." Whether or not a burst of VFO was associated with a chemical synaptic event, no change was seen in the frequency of the VFO itself [VFO/interictal event ($n = 690$) versus VFO alone ($n = 706$), 263.7 Hz versus 231.9 Hz; $P > 0.5$ Mann–Whitney rank-sum test].

The overt variability of synaptic inputs to pyramidal cells during field VFO may have been caused by the small number of cells sampled ($n = 8$ pyramids in total). However, as the high-frequency oscillations are a population event, the relative timing of synaptic inputs in individual neurons should reflect the network activity as a whole. We therefore examined the relationship between the phase of the VFO in interictal events and the peak of the corresponding components of compound EPSPs and IPSPs. No high-frequency intracellular correlate of field VFO could be seen in EPSP inputs to principal cells, so the analysis was not attempted on this measure. However, EPSPs onto FS interneurons have much faster kinetics, and these events did possess temporal structure which correlated with the concurrent field VFO (Fig. 4Ai). Recordings from FS interneurons showed a small compound EPSP during each interictal event studied. In each case no more than a single FS neuron action potential was elicited per interictal event, each coming off the largest of the components of the compound EPSP, suggesting that individual FS interneurons were not able to generate VFO alone during epileptic activity in the patients tested. Hyperpolarizing FS cells to −70 mV (Fig. 4Aii) permitted quantification of the peak of each component of the compound EPSP with respect to the accompanying period of field VFO. This revealed a strong phase locking of excitatory inputs to FS interneurons with the field VFO, but that peak EPSPs followed the peak negativity in the
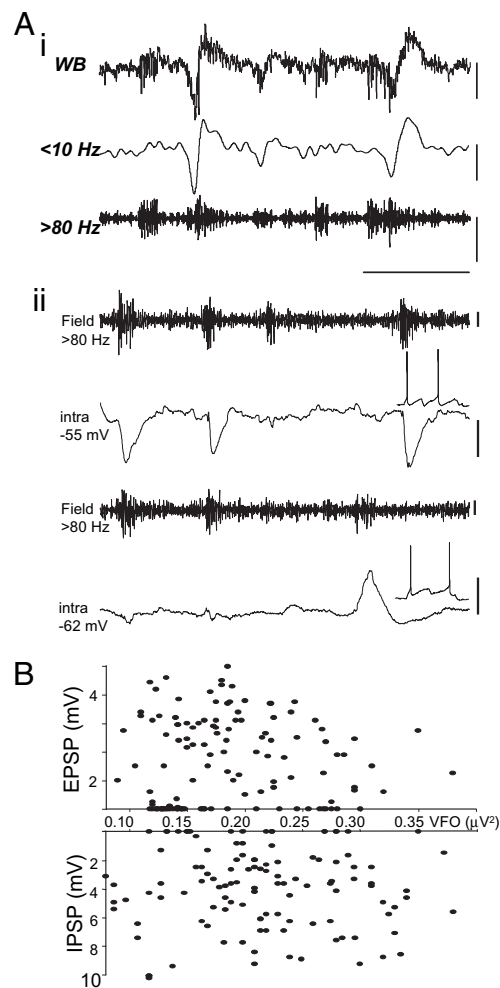

Fig. 3. The magnitude of synaptic excitation and inhibition in principal neurons is not correlated with VFO amplitude. (Ai) Example traces demonstrate the variability in the relationship between population VFO/pHFO occurrence and lower-frequency wave (spike) in local field potentials. (Aii) Principal neuron EPSPs and IPSPs also showed a variable occurrence with respect to field VFO/pHFO. IPSPs were recorded from artificially depolarized pyramidal cells (intra, −55 mV); EPSPs were recorded from resting membrane potential (intra, −62 mV). Note the varying amplitude and occurrence of failures of both EPSPs and IPSPs. [Scale bars, (Ai) 100 μV (WB, 10 Hz), 50 μV (>80 Hz); (Aii) 10 μV (field), 5 mV (intra, −55), 2 mV (intra, −62), 200 ms.] (B) Graphs illustrate the lack of significant relationship of both EPSPs and IPSPs in principal neurons with the amplitude of the concomitantly recorded VFO for each interictal discharge analyzed (126 for EPSPs, 116 for IPSPs).

field VFO, in each period, by a median of 2.7 ms (IQR 1.8–2.9 ms, $n = 200$ events from 3 interneurons).

The interneurons sampled again only reflect a small fraction of the possible sources of GABAergic input to principal cells. We therefore looked for any fine-scale temporal correlate in the compound inhibitory synaptic events reflecting all inhibitory neuronal outputs that converge onto regular spiking (RS) pyramidal neurons (Fig. 4Bi). The initial rise and peak of IPSPs revealed a very small correlate of the accompanying field VFO which could be revealed by high pass filtering. These filtered events were cross-correlated with the field VFO to assess any temporal relationship. The phase relationship between IPSP components and field VFO was very weak, with a median lag of 4.6 ms (IQR 3.2–5.2 ms, $n = 120$ events from 5 cells) (Fig. 2Bii). These data suggested that interneuron recruitment was not robust during interictal discharges, reflecting the variability in IPSP amplitudes accom-
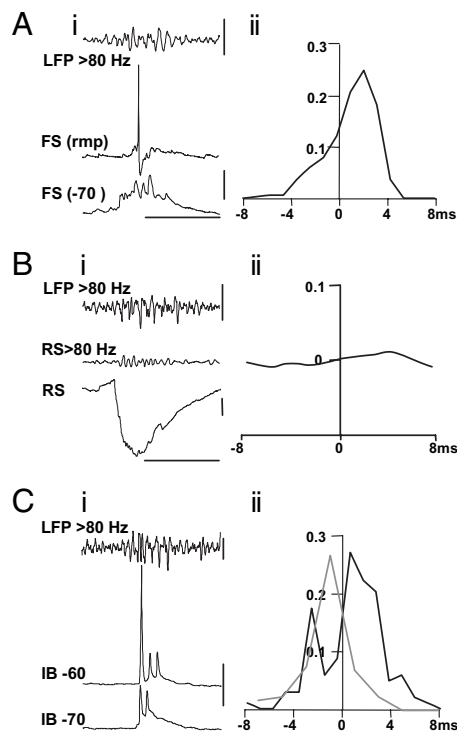
Fig. 4. Intracellular behavior of FS interneurons, RS and IB pyramidal cells in relation to VFO. (*Ai*) Concurrent recording from a superficial layer FS neocortical interneuron at resting membrane potential (−64 mV) and filtered (>80 Hz) LFP spontaneous VFO illustrates the lack of high-frequency output during the field VFO. In contrast, the compound EPSPs received by these FS interneurons during VFO displayed overt high-frequency activity at the field VFO frequency. (*Aii*) Graph shows the timing of FS interneuronal EPSP peaks with respect to the trough (maximum deflection) of each period of the VFO field potential waveform (n = 200 events from 3 interneurons). Note the clear lag (2.7 ms median) between VFO maximum deflection and the peak of the FS cell EPSP. (*Bi*) Recordings from an RS principal neuron receiving a predominantly inhibitory synaptic input during each interictal discharge. High pass filtering revealed a low-amplitude, high-frequency component to this input. (*Bii*) Cross-correlation analysis of the high pass filtered field potential and intracellular signal revealed only a very weak correlation between VFO activity and the high-frequency component of the IPSP, with a lag of 4.6 ms (median). (*Ci*) Intracellular recordings from a superficial layer intrinsically bursting (IB) neuron show bursts of spikelets (at −70 mV) or a mixture of full action potentials and spikelets coincident with the field VFO. (*Cii*) Cross-correlation of spikelets (black line) and full action potentials (gray line) versus the phase of the field VFO shows a slight phase lag for spikelets (<1 ms) and a phase-lead for action potentials (c.1 ms). [Scale bars, (*Ai*) 200 μV (upper), 20 mV (lower), 100 ms; (*Bi*) 100 μV, 2 mV, 100 ms; (*Ci*) 50 μV (upper), 10 mV (lower), 50 ms.]

panying interictal discharges. Furthermore, the timing of FS interneuronal EPSPs, and compound pyramidal cell IPSPs, indicated that inhibition was recruited by VFO, but not causal to it.

So what is generating the VFO/pHFO discharges that appear to underlie interictal discharges? Hippocampal interictal-like discharges in animal models are sensitive to gap junction conductance (39), and gap junctions between principal cells are critical for transformation from physiological rhythms to interictal activity in a computational model (35). Furthermore, transient bursts of VFO in field potential and pyramidal cell recordings are sensitive to a range of manipulations affecting gap junction conductance (23). We found intracellular correlates of such gap junctional communication between principal cells in six out of nine pyramidal cells recorded in the absence of drugs in epileptic tissue. Each showed brief bursts of activity associated with the field VFO, characterized by single full action potentials in a brief train of 2–5

spikelets (Fig. 4*C*). Full spikes had a clear "notch" in the rising phase, indicating that they were generated from spikelets. These spikelets were also tightly phase locked to the concurrently recorded VFO with a small median lag of 1.2 (IQR −0.3–2.4) ms (Fig. 4*Cii*). In contrast, full action potentials occurred with a phase lead of 1.5 (IQR −0.8–3.0) ms (Fig. 4*Cii*). These transient runs of spikelets persist after removal of all chemical synaptic transmission from the cortical column model, as long as gap junction conductance is high enough (Fig. S1*C*).

We next investigated the effects of reduced gap junction conductance on the occurrence of the field events themselves. Bath application of carbenoxolone (100–200 μM) abolished *both* the VFO and the slow envelope associated with interictal spikes in each slice tested (n = 5; Fig. 5). Wash-out of carbenoxolone after 60 min caused a return of interictal activity with embedded VFO. This result was in contrast to the effects of partial disinhibition (Fig. 2*B*), which abolished the slow envelope of the interictal discharge but preserved the VFO. Thus, the sensitivity of interictal events as a whole to gap junction conductance, and the presence of trains of spikelets, tightly phase locked to the field VFO in bursting cells, fits the model prediction that VFO is generated in nonsynaptic principal cell networks.

Discussion

Clinical observations of epileptiform activity *in situ* have suggested seizures may initiate in microdomains as small as 1 mm³ (33) or even less (40), and similar observations have been made in animal models (15). The present data reinforce this by demonstrating that spontaneous interictal activity in human epileptic neocortex is generated by highly localized neuronal networks, in the absence of ascending cortical input or neuromodulation, in vitro in brain slices less than 0.5 mm thick—approximately the width of a single cortical column (41). Biologically realistic computational models of single cortical columns containing only a few thousand neurons are capable of generating a rich array of physiological and epileptiform discharges (35), but what cellular and network mechanisms underlie interictal discharges?

Interictal sharp waves closely resemble physiological sharp waves, of which much more is known in terms of mechanism and function. Studies on the VFO component of sharp waves have concentrated on the activity of subsets of FS interneurons, with the observation that field VFOs (or ripples) are associated with transient synchronized discharge of FS interneurons (20, 42), mostly of the parvalbumin-expressing type (21). However, this does not mean that interneuron outputs have a causal relationship to the VFO. Indeed, unit recordings in rodent and human have shown that individual interneuron spikes lag behind the maximum deflection of each period of the field VFO by several milliseconds. In contrast, pyramidal cell units spike with near-zero phase relationship to the VFO (34, 42). This temporal pattern of pyramidal cell spiking leading interneuron excitatory synaptic input and subsequent spiking was also seen during VFO associated with interictal discharges in the present study.

Further evidence for a casual rather than causal role for interneurons in VFO generation comes from studies showing that sharp waves/interictal events with high-frequency components survive, and may even be enhanced by, GABA$_A$ receptor blockade (37, 39) and that interictal events with VFO are enhanced in mice lacking the gene for the main gap junction subunit coupling FS interneurons (39). Unlike studies on human subicular interictal discharges, which revealed a prominent role for depolarizing GABAergic events (43), neocortical interictal discharges are accompanied by normal, hyperpolarizing GABAergic events (44), and overt IPSPs are visible in pyramidal cells with membrane potentials as low as −65 mV in the present study. The data here also demonstrated that the slow component of interictal discharges was mediated by synaptic inhibition but that the VFO component could exist without this. Taken together, this evidence
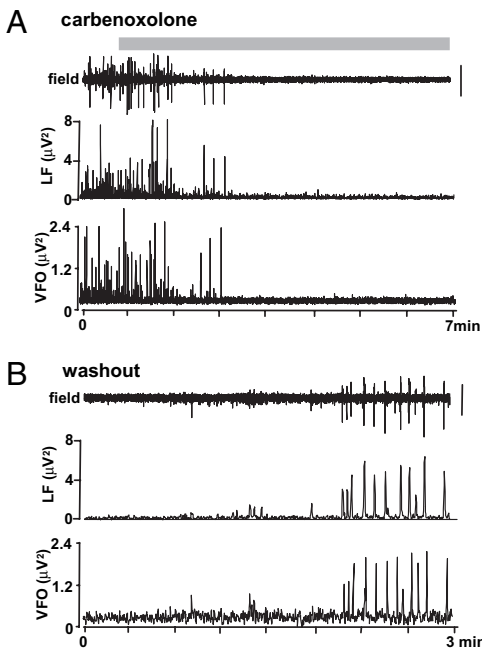
NEUROSCIENCE

Fig. 5. Reduced gap junction conductance with carbenoxolone reversibly abolished both interictal events and underlying VFO/pHFO. (*A*) Long time-course trace illustrates the action of the gap junction blocker carbenoxolone (200 μM; application denoted by gray bar), on spontaneous sharp wave and VFO behavior. The plots below denote the instantaneous peak amplitude value (for 200 ms sliding-windowed spectra) for low-frequency envelope of the interictal event (<20 Hz, LF) and the VFO itself (>80 Hz, VFO). (Scale bar, 100 μV.) (*B*) Wash-out of carbenoxolone rapidly restored both the spontaneous incidence of VFO and the low-frequency spike (wave) to near-control levels.

suggests that the low-frequency envelope of sharp waves and interictal spikes is generated for the most part by a population IPSP, but that this component is secondary to a process involving excitatory neuronal spike generation.

Clues to what this excitatory neuronal spike process may be come from studies on pyramidal cell spike patterns in non-synaptic conditions. Brief bursts of full action potentials and spikelets occur spontaneously in the absence of synaptic transmission in pyramidal cells (23). The process closely resembles the pattern of spike discharges seen in principal cells during sharp waves, with the spikelets, and accompanying antidromic full spikes, being generated by ectopic activity in axons propagating through a gap-junctionally coupled axon plexus (24, 25). Bursting neurons in temporal cortex in the present study revealed this characteristic pattern of full spike and spikelet trains was coincident with the field VFO. Furthermore, the full spikes were phase locked to the peak of each VFO wave with a lag of only c.1 ms—several milliseconds less than the lag for excitatory input, and subsequent spiking, in interneurons. Reduced gap junction conductance with carbenoxolone has been shown before to abolish interictal-like events in hippocampus (38) and to abolish both the VFO and the slow envelope of the interictal discharge in human temporal cortex here. Whereas carbenoxolone has also been shown to have effects on NMDA receptors (45), this subtype of glutamatergic receptor is not involved in human interictal discharges (44), an observation also seen with the present data set. Thus, the VFO/pHFO component of the interictal discharges seen appeared to be generated by trains of population spikes from synchronous action potential generation in a subset of gap-junctionally coupled local axons.

The present data indicate that the VFO/pHFO is capable of recruiting both recurrent excitatory synaptic connections and also

feedback inhibitory synaptic activity from interneurons. This pattern of events closely resembles the mechanisms implicated in physiological sharp wave generation (20, 21, 27, 46). Thus, it is not clear from this whether interictal discharges are a pathological process in epilepsy at all. However, the synaptic events associated with VFO in interictal discharges were heterogeneous (Fig. 3), with the degree of recruitment of both synaptic excitation and inhibition being extremely variable from interictal spike to interictal spike in each patient. This is in contrast to observations of physiological sharp waves where the majority of local pyramidal cells receive robust, stereotyped synaptic inhibition on each event (37). Furthermore, the relatively poor recruitment of interneuron spiking during each interictal event also contrasts with the intense interneuronal spike discharges seen during physiological sharp waves. This suggests that, whereas both events may be precipitated by principal cell axonal plexus activity, this excitation only weakly and erratically activates local inhibition—a situation akin to that described previously in the "dormant basket cell" hypothesis of epileptogenesis (47).

Given that interictal events are seen to immediately precede ictal events in a number of epilepsies (30), it is feasible that these apparently "ictogenic" events may represent extreme cases within this pattern of weak and variable interneuron recruitment, with nonsynaptic network events strongly recruiting recurrent excitation while failing to recruit concurrent inhibition. Such a network state would be expected to lead to iterative activation of recurrent networks typical of ictaform events in neocortex, as seen for fast runs during seizures in cat (48, 49). Thus, the enormous variability in recruiting chemical synaptic events during interictal discharges may serve to delineate these from physiological sharp waves and may constitute a primary pathology associated with ictogenesis in neocortical epilepsies.

Methods

Patients. Data were taken from 11 patients (aged 11–54 yr) with medically intractable temporal lobe epilepsy undergoing elective neurosurgery for surgical resection (see Table S1 for details). All patients gave their informed consent for the use of the resected brain tissue before surgery. This study was approved by the South Tees Local Research Ethics Committee (06/Q1003/51) and had clinical governance approved by the Newcastle Upon Tyne Hospitals NHS Trust (CM/PB/3707). Control tissue, not associated with clinical diagnosis of—or any manifestation of—epilepsy, was taken from temporal cortex removed to gain access for surgical treatment in 7 patients (6 male, 1 female, mean age 54.7 years). Surgery was carried out for glioblastoma (5), temporal hamartoma (1), and temporal metastasis (1).

In Vitro Electrophysiology. Human slices were derived from material removed as part of surgical treatment of medically intractable cortical epilepsy from the left and right temporal regions with written informed consent of the patients. Anesthesia was induced with intravenous remifentanil with/without alfentanil (0.2–0.4 μg/kg, 1 mg/kg, respectively). At induction a bolus dose of propofol (1–2 mg/kg) was administered intravenously. The patient also received a muscle relaxant, vecuronium (0.1 mg/kg). Anesthesia was maintained with remifentanil, oxygen, and desflurane at minimum alveolar concentration (MAC) volume of 0.5–1. Resected tissue was immediately transferred to sucrose-containing artificial cerebrospinal fluid (sACSF) containing (mM): 252 sucrose, 3 KCl, 1.25 NaH_2PO_4, 2 $MgSO_4$, 2 $CaCl_2$, 24 $NaHCO_3$ and 10 glucose. Neocortical slices containing all layers were cut at 450 μm (Microm HM 650 V), incubated at room temperature for 20–30 min, then transferred to a standard interface recording chamber at 34–36°C perfused with oxygenated ACSF containing (mM): 126 NaCl, 3 KCl, 1.25 NaH_2PO_4, 1 $MgSO_4$, 1.2 $CaCl_2$, 24 $NaHCO_3$ and 10 glucose. The time between resection and slice preparation was <1 min. Extracellular recordings (5–500 Hz) were conducted with ACSF-filled glass microelectrodes (2 MΩ). Intracellular recordings (DC-1 kHz) were taken using sharp electrodes (2 M KAc, 40–120 MΩ). VFO was separated from the slow envelope of interictal spikes by high pass filtering (>80 Hz). The slow envelope was quantified after low pass filtering (<20 Hz).

VFO Detection. Data were filtered with an equiripple Finite Impulse Response (FIR) filter, with band pass settings to isolate ripple (80–200 Hz), fast ripple

(200–500 Hz), or both types (80–500 Hz) of activity. To detect significant levels of ripple and fast ripple activity, we used three methods: (*i*) the filtered data were simply thresholded at the mean + 3 standard deviations (SDs) of the data; (*ii*) Teager energy [using the Kaiser method (50, 51)] was calculated for all points in the data as (x(n) (2) −(x(n − 1) × x(n + 1)); a simple threshold of global mean + 2 SDs of the data was then used; and (*iii*) line length (x(n) − x(n − 1)) (33) was calculated for all points in the data, and the global mean + 2 SDs were employed to threshold the data. None of the methods performed any better or worse in comparisons with "by-eye" detection.

Model Construction. The network model followed principles outlined in ref. 9, and a modified version was used of the simulation program described therein. The present network contained 4750 multicompartment cortical "neurons," each with a soma, axon initial segment, and several dendrites, and containing a variety of intrinsic Na$^+$, K$^+$, Ca^{2+}, and anomalous rectifier conductances. There were 2000-layer 5-tufted intrinsically bursting (IB) neurons, as well as deep and superficial RS pyramidal cells, superficial fast rhythmic bursting pyramidal cells, spiny stellate cells, and four types of interneuron (basket, axo-axonic, low threshold spiking, neurogliaform). Cells were inter-connected by excitatory synapses (with AMPA receptors), inhibitory synapses (with GABA$_A$ receptors), axonal gap junctions between homologous types of excitatory neurons, and dendritic gap junctions between homologous types of interneurons. Collective behavior was most dependent on gap junctions between layer 5 IB cells; there were 2500 of these, so that each cell was coupled to 2.5 others, on average. Collective behavior was induced by a 50 ms transient opening of the gap junctions between IB cells: the conductance rose linearly from 0.0 to 8.0 nS, and then declined linearly. The simulation program, interactBAIX.f, was in Fortran and was run on 27 nodes of a parallel computer at the IBM T.J. Watson Research Center, with the MPI (message passing interface) parallel environment and AIX operating system. The program is available on request to rtraub@us.ibm.com.

1. Crone NE, Miglioretti DL, Gordon B, Lesser RP (1998) Functional mapping of human sensorimotor cortex with electrocorticographic spectral analysis. II. Event-related synchronization in the gamma band. *Brain* 121:2301–2315.
2. Curio G, et al. (1994) Localization of evoked neuromagnetic 600 Hz activity in the cerebral somatosensory system. *Electroencephalogr Clin Neurophysiol* 91:483–487.
3. Edwards E, Soltani M, Deouell LY, Berger MS, Knight RT (2005) High gamma activity in response to deviant auditory stimuli recorded directly from human cortex. *J Neurophysiol* 94:4269–4280.
4. Canolty RT, et al. (2006) High gamma power is phase-locked to theta oscillations in human neocortex. *Science* 313:1626–1628.
5. Niedermeyer E (2005) Ultrafast EEG activities and their significance. *Clin EEG Neurosci* 36:257–262.
6. Grenier F, Timofeev I, Steriade M (2003) Neocortical very fast oscillations (ripples, 80–200 Hz) during seizures: Intracellular correlates. *J Neurophysiol* 89:841–852.
7. Rodin E (2005) Paper recordings of ultrafast frequencies in experimental epilepsy. *Clin EEG Neurosci* 36:263–270.
8. Traub RD, et al. (2001) A possible role for gap junctions in generation of very fast EEG oscillations preceding the onset of, and perhaps initiating, seizures. *Epilepsia* 42:153–170.
9. Traub RD, et al. (2005a) Single-column thalamocortical network model exhibiting gamma oscillations, sleep spindles, and epileptogenic bursts. *J Neurophysiol* 93:2194–2232.
10. Bragin A, Engel J, Jr, Wilson CL, Fried I, Buzsáki G (1999a) High-frequency oscillations in human brain. *Hippocampus* 9:137–142.
11. Bragin A, Engel J, Jr, Wilson CL, Fried I, Mathern GW (1999b) Hippocampal and entorhinal cortex high-frequency oscillations (100–500 Hz) in human epileptic brain and in kainic acid-treated rats with chronic seizures. *Epilepsia* 40:127–137.
12. Staba RJ, Wilson CL, Bragin A, Fried I, Engel J, Jr (2002) Quantitative analysis of high-frequency oscillations (80–500 Hz) recorded in human epileptic hippocampus and entorhinal cortex. *J Neurophysiol* 88:1743–1752.
13. Staba RJ, et al. (2004) High-frequency oscillations recorded in human medial temporal lobe during sleep. *Ann Neurol* 56:108–115.
14. Jirsch JD, et al. (2006) High-frequency oscillations during human focal seizures. *Brain* 129:1593–1608.
15. Bragin A, Mody I, Wilson CL, Engel J, Jr (2002a) Local generation of fast ripples in epileptic brain. *J Neurosci* 22:2012–2021.
16. Bragin A, et al. (2002b) Interictal high-frequency oscillations (80–500 Hz) in the human epileptic brain: Entorhinal cortex. *Ann Neurol* 52:407–415.
17. Ochi A, et al. (2007) Dynamic changes of ictal high-frequency oscillations in neocortical epilepsy: Using multiple band frequency analysis. *Epilepsia* 48:286–296.
18. Jacobs J, et al. (2008) Interictal high-frequency oscillations (80–500 Hz) are an indicator of seizure onset areas independent of spikes in the human epileptic brain. *Epilepsia* 49:1893–1907.
19. Wilson MA, McNaughton BL (1994) Reactivation of hippocampal ensemble memories during sleep. *Science* 265:676–679.
20. Buzsáki G, Horváth Z, Urioste R, Hetke J, Wise K (1992) High-frequency network oscillation in the hippocampus. *Science* 256:1025–1027.
21. Klausberger T, et al. (2003) Brain-state- and cell-type-specific firing of hippocampal interneurons in vivo. *Nature*, 421:844–848, and erratum (2006) 441:902.
22. Maier N, Nimmrich V, Draguhn A (2003) Cellular and network mechanisms underlying spontaneous sharp wave-ripple complexes in mouse hippocampal slices. *J Physiol* 550:873–887.
23. Draguhn A, Traub RD, Schmitz D, Jefferys JG (1998) Electrical coupling underlies high-frequency oscillations in the hippocampus in vitro. *Nature* 394:189–192.
24. Traub RD, et al. (2002) Axonal gap junctions between principal neurons: A novel source of network oscillations, and perhaps epileptogenesis. *Rev Neurosci* 13:1–30.
25. Schmitz D, et al. (2001) Axo-axonal coupling. A novel mechanism for ultrafast neuronal communication. *Neuron* 31:831–840.
26. Hamzei-Sichani F, et al. (2007) Gap junctions on hippocampal mossy fiber axons demonstrated by thin-section electron microscopy and freeze fracture replica immunogold labeling. *Proc Natl Acad Sci USA* 104:12548–12553.
27. Ylinen A, et al. (1995) Sharp wave-associated high-frequency oscillation (200 Hz) in the intact hippocampus: Network and intracellular mechanisms. *J Neurosci* 15:30–46.
28. Akiyama T, et al. (2005) Focal cortical high-frequency oscillations trigger epileptic spasms: Confirmation by digital video subdural EEG. *Clin Neurophysiol* 116:2819–2825.
29. Khosravani H, et al. (2009) Spatial localization and time-dependant changes of electrographic high frequency oscillations in human temporal lobe epilepsy. *Epilepsia* 50:605–616.
30. Roopun AK, et al. (2009) Detecting seizure origin using basic, multiscale population dynamic measures: Preliminary findings. *Epilepsy Behav* 14 (Suppl 1):39–46.
31. Worrell GA, et al. (2004) High-frequency oscillations and seizure generation in neocortical epilepsy. *Brain* 127:1496–1506.
32. Urrestarazu E, Chander R, Dubeau F, Gotman J (2007) Interictal high-frequency oscillations (100–500 Hz) in the intracerebral EEG of epileptic patients. *Brain* 130:2354–2366.
33. Worrell GA, et al. (2008) High-frequency oscillations in human temporal lobe: Simultaneous microwire and clinical macroelectrode recordings. *Brain* 131:928–937.
34. Le Van Quyen M, et al. (2008) Cell type-specific firing during ripple oscillations in the hippocampal formation of humans. *J Neurosci* 28:6104–6110.
35. Traub RD, et al. (2005b) Transient depression of excitatory synapses on interneurons contributes to epileptiform bursts during gamma oscillations in the mouse hippocampal slice. *J Neurophysiol* 94:1225–1235.
36. Jacobs J, et al. (2009) High frequency oscillations in intracranial EEGs mark epileptogenicity rather than lesion type. *Brain* 132:1022–1037.
37. Nimmrich V, Maier N, Schmitz D, Draguhn A (2005) Induced sharp wave-ripple complexes in the absence of synaptic inhibition in mouse hippocampal slices. *J Physiol* 563:663–670.
38. Huberfeld G, et al. (2007) Perturbed chloride homeostasis and GABAergic signaling in human temporal lobe epilepsy. *J Neurosci* 27:9866–9873.
39. Pais I, et al. (2003) Sharp wave-like activity in the hippocampus in vitro in mice lacking the gap junction protein connexin 36. *J Neurophysiol* 89:2046–2054.
40. Schevon CA, et al. (2008) Microphysiology of epileptiform activity in human neocortex. *J Clin Neurophysiol* 25:321–330.
41. Mountcastle VB (1978) An organization principle for cerebral function: the unit module and the distributed system, in *The Mindful Brain*, eds Edelman GM, Mountcastle VB (MIT Press, Cambridge, MA), pp 7–50.
42. Csicsvari J, Hirase H, Czurkó A, Mamiya A, Buzsáki G (1999) Oscillatory coupling of hippocampal pyramidal cells and interneurons in the behaving rat. *J Neurosci* 19:274–287.
43. Cohen I, Navarro V, Clemenceau S, Baulac M, Miles R (2002) On the origin of interictal activity in human temporal lobe epilepsy in vitro. *Science* 298:1418–1421.
44. Köhling R, et al. (1998) Spontaneous sharp waves in human neocortical slices excised from epileptic patients. *Brain* 121:1073–1087.
45. Chepkova AN, Sergeeva OA, Haas HL (2008) Carbenoxolone impairs LTP and blocks NMDA receptors in murine hippocampus. *Neuropharmacology* 55:139–147.
46. Traub RD, Bibbig A (2000) A model of high-frequency ripples in the hippocampus based on synaptic coupling plus axon-axon gap junctions between pyramidal neurons. *J Neurosci* 20:2086–2093.
47. Sloviter RS (1991) Permanently altered hippocampal structure, excitability, and inhibition after experimental status epilepticus in the rat: The "dormant basket cell" hypothesis and its possible relevance to temporal lobe epilepsy. *Hippocampus* 1:41–66.
48. Steriade M (2003) *Neuronal Substrates of Sleep and Epilepsy* (MIT Press, Cambridge, MA), pp 191–271.
49. Steriade M, Amzica F, Neckelmann D, Timofeev I (1998) Spike-wave complexes and fast components of cortically generated seizures. II. Extra- and intracellular patterns. *J Neurophysiol* 80:1456–1479.
50. Kaiser JF (1990) On a simple algorithm to calculate the "energy" of a signal. *Proceedings—ICASSP, IEEE International Conference on Acoustics, Speech and Signal Processing* (IEEE Publishing, Los Alamitos, CA), pp 381–384.
51. Nelson R, et al. (2006) Detection of high frequency oscillations with Teager energy in an animal model of limbic epilepsy. *Conf Proc IEEE Eng Med Biol Soc* (IEEE Publishing, Los Alamitos, CA), 1:2578–2580.

NEUROSCIENCE